https://doi.org/10.5194/angeo-2020-91
Preprint. Discussion started: 13 January 2021

Annales Geophysicae Discussions

Detection of Kelvin-Helmholtz billows over the National Capital Region of India using SODAR

Nishant Kumar[a], Kirti Soni[b*], Ravinder Agarwal[a]
[a]*Thapar Institute of Engineering and Technology, Patiala*
[b]*CSIR-National Physical Laboratory, New Delhi, (India)*

[*]*Email: - 2006.kirti@gmail.com*

Abstract

Kelvin-Helmholtz billows (KHB) have been investigated in the Atmospheric Boundary layer (ABL) using Mono-static SODAR (Sound Detection And Ranging) designed and developed by CSIR-National Physical Laboratory, New Delhi over the capital region Delhi of India. KH billows are a primary cause of mixing in stably stratified conditions and hence have been studied widely by researchers by using ground-based and remote sensing methods. About ninety cases of KHBs observed in SODAR echograms from March 2019 to November 2019 in the ABL. Trains of K-H billows lasting from thirty minutes to various minutes were frequently detected in the lower portion of the troposphere (ABL), creating in a statically stable ABL. Most recognised billows are round the resolution limit of SODAR. Additionally, several of the cases contain billows with extremely varied amplitudes and shapes. The most significant number of episodes observed in the October months were related with the morning growth of the inversion.

Keywords: Kelvin–Helmholtz billows, Turbulence, SODAR, Atmospheric Boundary Layer

https://doi.org/10.5194/angeo-2020-91
Preprint. Discussion started: 13 January 2021

Annales Geophysicae Discussions

1. Introduction

The rotation of air around the Earth's surface generates resistance in a thin layer approximately one-tenth of the troposphere ensuing in an Atmospheric Boundary Layer (ABL) (Garratt, 1994; Bradley, 2007). Due to the thermal condition of the atmosphere and the effect of Coriolis force owing to the Earth's rotation, ABL has a force of buoyancy (Stull, 2012). Turbulence in ABL is responsible for the transportation of heat, momentum, and pollutants. Consequently, ABL is a turbulent boundary layer in revolving heavily stratified liquid. The ABL width varies from 0.1 to 3 km (Asimakopoulos et al., 1976). The time scales are of the order of one hour for the variation to happen but not for steadiness to be established in the ABL height. The internal structure of the ABL is controlled by the large -scale motion of the atmosphere, and therefore it also describes the scales of turbulence (Aggarwal et al., 1980; Caughey, 1984). Though, turbulence breaks down the large-scale motions and disperses them. The ABL has a significant influence on the performance of the atmosphere and activities concerning the representation of the atmosphere, for example, climate modelling and numerical weather prediction, cannot succeed without the boundary layer study (Singal and Aggarwal, 1979; Beyrich, 1993; Emeis et al., 2008). According to Stull (2012) in the structure of ABL when stratocumulus topped, a mixed layer passes over the warmer ground surface. The thermals growing from the ground meet the descending cooling thermals produced as a result of radiative cooling at above the clouds. Thus, the convection process takes place, and the turbulence has generated. In this sense, the turbulence in the mixed layer is caused by convection (Kallistratova et al., 2019).

Strong free shear is produced by the air that flows through the top layer and causes turbulence to occur. However, the turbulence here is thought to be associated with Clear Air Turbulence (CAT) and is produced by the breaking down of the Kelvin-Helmholtz Billows (KHB) (Sekioka, 1970; Browning, 1971; Klaassen and Peltier, 1985a, 1985b; De et al., 1996; Blumen et al., 2001; Lyulyukin et al., 2013). The static stability also modifies the forms of turbulent eddies. Under statically unstable conditions with rising thermals, the largest eddies are anisotropic, with immense turbulent energy in the vertical motion component rather than in the horizontal part (Garratt, 1994; Stull, 2012). The continuous exhaust of smoke from industries and vehicles spreads throughout the atmosphere; however, the direction of movement of smoke is horizontal rather than vertical. When the shear in laminar flow between the masses (e.g., between the cold air below and the warm air above) rises to the point where the flow again

https://doi.org/10.5194/angeo-2020-91
Preprint. Discussion started: 13 January 2021

becomes unstable, the onset of turbulence increases as Kelvin-Helmholtz (KH) instability on the interface.

First, small waves rise that increase in amplitude and curl over on themselves. If sufficient moisture is present in the atmosphere, the cloud can form in the rising parts of each curl, giving a pattern that looks like waves that break from the sea when viewed from side to side. The structures of the KHB in the raised inversion layers above the convection have revealed in the late 1960s by using SODAR and RADAR (Singh et al., 1999; Van and Gostiaux, 2010). Recently, the KHB in the rising inversions was also found by using LIDAR (Lyulyukin et al., 2019). These structures, such as KHB in the form of ponytails, are particularly evident in SODAR echograms.

The purpose of this study is an experimental investigation of internal shear-induced waves due to a KHB. It is an essential problem for the study of stably-stratified ABL, the predication of CAT, local wind shear, temperature inversions, storms, and necessary for aviation safety. In this study, the results of long-term continuous SODAR (SOnic Detection And Ranging) measurements used to obtain the statistics on the occurrence of KHB, their duration, amplitude, time and wavelength, etc. Statistical comparisons of some parameters of the ABL obtained from SODAR measurements, with KHB features have made.

2. Measurement Site and Equipment

The SODAR system was developed by CSIR-NPL, New Delhi. The details about data acquisition and instrumentations are described in Singal and Aggarwal (1979), Kumar et al. (2017b, 2019b). The NPL SODAR is a new generation, high-power, highly sensitive monostatic SODAR system. The SODAR transmits sound signal into the atmosphere with periods of 100 ms at 2250 Hz and average acoustic power of 20 W in the vertical direction at a pulse recurrence rate of 4 s, restraining the maximum potential range to 1000 m, with the lowermost observation height of about 50 m and perpendicular resolution of about 17 m. The SODAR system was newly installed at CSIR-NPL (28.7041° N, 77.1025° E), and it has located in central in the homogeneous urban area of Delhi (Kumar et al., 2015, 2017a). SODAR provides continuous vertical profile of the temperature structure parameter C_T^2 and also a clear ABL structure (Petenko et al., 2020).

https://doi.org/10.5194/angeo-2020-91
Preprint. Discussion started: 13 January 2021

For the measurement of wind speed, wind direction, temperature and relative humidity at 20 m, the weather station of CSIR-NPL is furnished with the following equipment's and their technical information is summarised in Table 1:

Table 1: Meteorological Sensor Information

Instrument	Make	Accuracy
Combined Wind Sensor	Barani Design	± 0.032 m/s WS ± 1-degree WD
Digital Temperature and RH Data logger with Sensor	Sivara System	± 0.4 % RH ± 0.20 C Temperature

3. Results and Discussions

Considering the vastness of the SODAR measurements such as the spatial (vertical) structure of the ABL, it is nearly impossible to accommodate all the results and the outcomes in a single paper. Accordingly, the present experiment has been confined to the study of KHBs in the ABL performed during March 2019 to November 2019 in Delhi. The process of Convection development and early morning surface radiation inversion is best seen in summer and winter SODAR echograms, which were observed in early 1975 at CSIR-NPL, New Delhi (Singal and Aggarwal, 1979). SODAR gives the main structures of the spatio - temporal continuum of the thermal turbulence in the Delhi region. Fig. 1 provided the diurnal variation and different structures of the ABL. The primary regime can be defined as a "classical" twenty-four-hour pattern displaying alternation among stable (inversion in the evening and night-time, 1900 to 0009 IST) and unstable (convection in the daytime, 0009 to 1700 IST) stratification, with two transition periods about 0700–1000 IST and 1600–1800 IST. For this, local circulation is not clear; the wind pattern is characterised land breeze, with direction 250 to 300 degree. The diurnal behaviours of temperature and relative humidity are typical for fair-weather conditions. In the inversion layer wind speed profile display a repetitive growth with elevation, reaching an extreme at the topmost of the inversion layer. The wind speed and direction changes between 0930-1115 IST, due to breakdown of multilayer.

The example of KHB is presented in Fig. 2. This structural pattern is similar to a braid or herringbone pattern of K-H billows, with the periodicity of the braids is about 90-110 s. The braid slopes angle seems to be associated with the altitude dependency of the average flow speed in the wavy layer. Sound backscattering is found at small-scale turbulent temperature

https://doi.org/10.5194/angeo-2020-91
Preprint. Discussion started: 13 January 2021

inhomogeneity's (Gilman et al., 1946). The return signal intensity is directly related to the temperature structure parameter (Danilov et al., 1992; Kumar et al., 2020). Therefore, the SODAR echogram presented the mesoscale wave motions of small-scale temperature fluctuations (Choudhury and Mitra, 2004; Kumar et al., 2019a). The stratification conditions in the ABL are identified, using the well-recognized method defined in numerous studies. As per this method, an echogram pattern which looks as vertically prolonged KH billows is associated with stable (inversion) layer (Sun et al., 2015).

Approximately 90 patterns of the occurrences of the billows were recognized by visual inspection of echograms from March 2019 to November 2019. Multiple billows have been identified about the resolution limit of the SODAR. Additionally, most patterns involve billows with extremely varied amplitudes and shapes, e.g., during the lifting of the inversion layer billow amplitude can rise from 100 to 300 m at the morning.

Following conditions are applied to select appropriate samples for analysis:

1. The train includes more than five well-pronounced billows of similar shape
2. The billows period is more than or equal to 100 s.
3. The amplitude of the billows varies within 35% limits.

Table 2: Number of KHBs episodes in 2019

	March	April	May	June	July	August	September	October	November
Rising Layer	13	10	14	8	5	8	6	10	14
KHBs All	1	4	4	3	0	0	0	5	4

The temporal analysis of the SODAR echogram is used to evaluate and compare the periods of the KHB structure during the inversion layer. The height of the time series of SODAR echograms is chosen to be within the segment with KHBs. There were 21 patterns in the dataset that satisfy the criteria defined above. Examples of SODAR echograms with clear KHB in the form of braids or inclined stripes are shown in Fig. 2. The monthly distribution of the number of such trains, is shown in Table 2. The most significant number of episodes seen in the October months were linked with the morning rise of the inversion support the assumption of a prominent role of convection in the formation of waves. But in reality, as will be presented below, it is not a "mechanical" effect of vertical convection motions, but the fact that static stability in the rising inversion layer is less than in the surface layer (Browning, 1971). Thus, the conditions for the existence of shear instabilities are observed.

https://doi.org/10.5194/angeo-2020-91
Preprint. Discussion started: 13 January 2021

Annales Geophysicae Discussions

SODAR echograms visualising the shape of the detected waves and averaged ABL height are presented in Fig (3). In Fig. (3) an example of the KHBs obtained at CSIR-NPL, New Delhi in the pre-monsoon period 12th March 2019, 26th April 2019, 25th May 2019, 14th June 2019 are shown. Clear KHB structures have seen in the pattern of the backscattered signal intensity in height-time coordinates. These echogram patterns confirmed the interpretation of the episode of KHB structure in the different weather conditions. Most of the selected cases with clear KHB occur at midnight (i.e., after midnight, Fig. 2). The significant change in the structure of wind velocity, temperature gradient within KHB is strongly associated (Klaasen and Peltier, 1985a, 1985b; De et al., 1996) and provided a braid shape of the turbulence structure.

For example, Fig. (4) demonstrates the composite forms of KHB and meteorological parameters. Fig. (4a) shows the temporal variation of the ABL height and meteorological parameter for the 24-hours. Fig. (4b) also shows the temporal variation of ABL height and meteorological parameters during the KHBs period. In a convection period of ABL, solar heating causes air near the surface to heat up and ascend through the atmosphere. Kline et al. (1967) performed laboratory experiments of turbulent free convection over a heated horizontal surface and observed that the temperature fluctuations showed periodic activity, characterised by alternating large swings and intermittent of quiescence. Other authors, Sparrow et al. (1970) purposed and visualised for the analytical models for heat transfer during forced and free convection i.e. these regular activities are due to mushroom-like structures of ascending hot fluid. Wilczak and Businger (1983) showed that surface layer plumes have diameters and depths on the order of the air in the surface layer. And advection velocity that is close to the wind speed averaged over their bottom.

Petenko et al. (2016) observed and suggested that the eddies responsible for plume-like structures are on the order of the Kolmogorov scale for smooth walls and roughness height for rough walls. Therefore, studied coherent turbulent structure during the KH billows period (including one day before and one day after the KH billows day). The high-resolution echograms give evidence of the regular periodic structure of slanted thin turbulent layers. This structural pattern resembles a braid (or herringbone) pattern of KH vortices in the layer. The cyclicity of the braids is about 70-120 s in the layer depending on the meteorological conditions (Petenko et al., 2020). The angle of the braid slopes seen to be associated with the height dependence of the mean flow speed in the wavy layer. The vorticity of the wind disturbance in KHBs can be clockwise or anticlockwise, depending on the average wind profile. A clear

https://doi.org/10.5194/angeo-2020-91
Preprint. Discussion started: 13 January 2021

Annales Geophysicae Discussions

example of the KHBs period has been observed in Fig. (4, 5). Fig. 4 represents the temporal echograms of ABL height with meteorological parameters during the KHBs and Fig. 5 provides the temporal data before and after the KHBs day. From Table 3, it is observed that the analysis of temporal echogram that convective periods have lower height after the KHBs, as compared to the previous day. Generation of KHBs also effects the next day convection. Petenko et al. (2016, 2020) presented that the KHB studies conducted by SODAR is limited by the time and spatial resolution of the Monostatic SODAR. In the formation of KH billows, it is observed from Fig. 4 (b) that as long as the temperature decreases and increases sufficiently with the wind speed and relative humidity, then curls is formed. After some time, the moisture decreases due to the increasing temperature, resulting in the gradual disappearance of the curls.

Table 3. Comparison Analysis of KH Billows Days

	Average			Maximum		Minimum	
	24 Hours	Convection Period	Inversion Period	Convection Period	Inversion Period	Convection Period	Inversion Period
18/05/2019 (Pre-KHB Days)	890±685	1605±155	280±55	1840	360	1350	210
19/05/2019 (KHB Days)	625±620	1162±125	245±65	1350	380	910	140
20/05/2019 (Post-KHB Days)	620±505	1195±155	210±50	1440	300	860	140

4. Conclusion

SODAR continuous measurements provide access to statistical information on the Kelvin-Helmholtz Billows. Several K-H billows events were recognized by visual inspection of the SODAR ecograms collected during the nine-month continuous monitoring of ABL in Delhi area. KHB trains ranging from thirty minutes to several hours were observed frequently in the lower portion of the troposphere (ABL), creating a stable ABL. The results of all the applied measurements presented in the figures provide information about the characteristic features of the phenomenon. The high-resolution echograms give evidence of the consistent periodic structure of slanted thin turbulent layers. This structural pattern looks like a braid shape of KH vortices in the layer. The periodicity of the braids is average (150 ± 10%) s in the layer depending on the meteorological conditions in Delhi region.

https://doi.org/10.5194/angeo-2020-91
Preprint. Discussion started: 13 January 2021

Annales Geophysicae Discussions Open Access EGU

Reference

Aggarwal, S. K., Singal, S. P., Kapoor, R. K., and Adiga, B. B.: A study of atmospheric structures using sodar in relation to land and sea breezes, Boundary-Layer Meteorology, **18(4)**, 361-371, 1980.

Asimakopoulos, D. N., Cole, R. S., Caughey, S. J., and Crease, B. A.: A quantitative comparison between acoustic sounder returns and the direct measurement of atmospheric temperature fluctuations, Boundary-Layer Meteorology, **10(2)**, 137-147, 1976.

Beyrich, F.: On the use of sodar data to estimate mixing height, Applied Physics Photophysics and Laser Chemistry, **57(1)**, 27-35, 1993.

Blumen, W., Banta, R., Burns, S. P., Fritts, D. C., Newsom, R., Poulos, G. S., and Sun, J.: Turbulence statistics of a Kelvin–Helmholtz billow event observed in the night-time boundary layer during the Cooperative Atmosphere–Surface Exchange Study field program, Dynamics of Atmospheres and Oceans, **34(2-4)**, 189-204, 2001.

Bradley, S.: Atmospheric acoustic remote sensing: principles and applications. CRC Press, 2007. eBook ISBN 9781420005288 https://www.taylorfrancis.com/books/9781420005288

Browning, K. A.: Structure of the atmosphere in the vicinity of large-amplitude Kelvin-Helmholtz billows, Quarterly Journal of the Royal Meteorological Society, **97(413)**, 283-299, 1971.

Caughey, S.J.: Observed characteristics of the atmospheric boundary layer, In Atmospheric turbulence and air pollution modelling, 107-158, 1984. Springer, Dordrecht.

Choudhury, S., and Mitra, S.: A connectionist approach to SODAR pattern classification, IEEE Geoscience and Remote Sensing Letters, **1(2)**, 42-46, 2004.

Danilov, S. D., Gur'yanov, A. E., Kallistratova, M. A., Petenko, I. V., Singal, S. P., Pahwa, D. R., and Gera, B. S.: Acoustic calibration of sodars, Measurement Science and Technology, **3(10)**, 1001-1010, 1992.

De, S. I. P. D., Fernando, H. J. S., Eaton, F., and Hebert, D.: Evolution of Kelvin-Helmholtz billows in nature and laboratory, Earth and Planetary Science Letters, **143(1-4)**, 217-231, 1996.

Emeis, S., Schäfer, K., and Münkel, C.: Surface-based remote sensing of the mixing-layer height–a review, Meteorologische Zeitschrift, **17(5)**, 621-630, 2008.

Garratt, J. R.: The atmospheric boundary layers, Earth-Science Reviews, **37(1-2)**, 89-134, 1994.

Gilman, G. W., Coxhead, H. B., and Willis, F. H.: Reflection of sound signals in the troposphere, The Journal of the Acoustical Society of America, **18(2)**, 274-283, 1946.

Kallistratova, M., Petenko I., Kouznetsov R., Kuznetsov D., Lyulyukin V., and Perepelkin V.: Kelvin-Helmholtz billows in rising morning inversions, In IOP Conference Series: Earth and Environmental Science, **231(1)**, 012025 (1-9), 2019.

Klaassen, G. P., and Peltier, W. R.: Evolution of finite amplitude Kelvin–Helmholtz billows in two spatial dimensions, Journal of the atmospheric sciences, **42(12)**, 1321-1339, 1985a.

Klaassen, G. P., and Peltier, W. R.: The onset of turbulence in finite-amplitude Kelvin–Helmholtz billows, Journal of Fluid Mechanics, **155**, 1-35, 1985b.

Kline, S. J., William, C. R., Schraub, F. A., and Runstadler, P. W.: The structure of turbulent boundary layers, Journal of Fluid Mechanics, **30(4)**, 741-773, 1967.

Kumar, N., Parmar, K. S., Soni, K., Garg, N., and Agarwal, R.: Prediction of ventilation coefficient, using a conjunction model of wavelet-Neuro-fuzzy Model: A Case Study Delhi, India, Academia Journal of Scientific Research, **3(12)**, 184-191, 2015.

Kumar, N., Soni, K., and Agarwal, R.: A comprehensive study of different feature selection methods and machine-learning techniques for SODAR structure classification, Modeling Earth Systems and Environment, **6**, 1-12, 2020. https://doi.org/10.1007/s40808-020-00872-0

Kumar, N., Soni, K., Agarwal, R., and Singh, M.: SODAR as a diagnostics tool for urban air-quality and health care system, Journal of Acoustical Society of India, **44(4)**, 213-222, 2017a.

Kumar, N., Soni, K., Agarwal, R., and Singh, M.: Performance of Acoustic Sounder and analysis of various features of Atmospheric Boundary Layer height during extreme weather conditions, In 2019 URSI Asia-Pacific Radio Science Conference (AP-RASC), pp. 1-1. IEEE, 2019a.

Kumar, N., Soni, K., Agarwal, R., and Singh, M.: Preliminary analysis of operating conditions of acoustic sounder (SODAR) before the installation, The Journal of the Acoustical Society of America, **146(4)**, 2997-2998, 2019b.

Kumar, N., Soni, K., Garg, N., Agarwal, R., Saha, D., Singh, M., and Singh, G.: SODAR pattern classification and its dependence on meteorological parameters over a semiarid region of India, International Journal of Remote Sensing, **38(11)**, 3466-3482, 2017b.

Lyulyukin, V., Kallistratova, M., Zaitseva, D., Kuznetsov, D., Artamonov, A., Repina, I., Petenko, I., Kouznetsov, R., and Pashkin, A.: Sodar observation of the ABL structure and waves over the Black Sea offshore site, Atmosphere, **10(12)**, 811 (1-16), 2019.

Lyulyukin, V., Kouznetsov, R., and Kallistratova, M.: The composite shape and structure of braid patterns in Kelvin–Helmholtz billows observed with a sodar, Journal of Atmospheric and Oceanic Technology, **30(12)**, 2704-2711, 2013.

Petenko, I., Argentini, S., Casasanta, G., Genthon, C., and Kallistratova, M.: Stable surface-based turbulent layer during the polar winter at Dome C, Antarctica: Sodar and in situ observations, Boundary-Layer Meteorology, **171(1)**, 101-128, 2019.

Petenko, I., Argentini, S., Casasanta, G., Kallistratova, M., Sozzi, R., and Viola, A.: Wavelike structures in the turbulent layer during the morning development of convection at Dome C, Antarctica, Boundary-Layer Meteorology, **161(2)**, 289-307, 2016.

Petenko, I., Casasanta, G., Bucci, S., Kallistratova, M., Sozzi, R., and Argentini, S.: Turbulence, Low-Level Jets, and Waves in the Tyrrhenian Coastal Zone as Shown by Sodar, Atmosphere, **11(1)**, 28(1-35), 2020.

Sekioka, M.: Application of Kelvin-Helmholtz instability to clear air turbulence, Journal of Applied Meteorology, **9(6)**, 896-899, 1970.

Singal, S. P., and Aggarwal, S. K.: Sodar & Radiosonde Studies of Thermal Structure of the Lower Atmosphere at Delhi, Indian Journal of Radio & Space Physics, **8**, 76-81, http://nopr.niscair.res.in/handle/123456789/37079, 1979.

Singh, S., Mahajan, K. K., Choudhary, R. K., and Nagpal, O. P.: Detection of Kelvin-Helmholtz instability with the Indian mesosphere-stratosphere-troposphere radar: A case study, Journal of Geophysical Research: Atmospheres, **104 (D4)**, 3937-3945, 1999.

Sparrow, E. M., Husar, R. B., and Goldstein, R. J.: Observations and other characteristics of thermals, Journal of Fluid Mechanics, **41(4)**, 793-800, 1970.

Stull, R. B.: An introduction to boundary layer meteorology. **Vol. 13**. Springer Business Media. eBook ISBN 978-94-009-3027-8 DOI 10.1007/978-94-009-3027-8, 2012.

Sun, J., Nappo, C. J., Mahrt, L., Belušić, D., Grisogono, B., Stauffer, D. R., Pulido, M., et al.,: Review of wave-turbulence interactions in the stable atmospheric boundary layer, Reviews of geophysics, **53(3)**, 956-993, 2015.

Van, H. H., and Gostiaux, L.: A deep-ocean Kelvin-Helmholtz billow train, Geophysical Research Letters, **37(3)**, L03605(1-5), 2010.

https://doi.org/10.5194/angeo-2020-91
Preprint. Discussion started: 13 January 2021

Wilczak, J. M., and Businger, J. A.: Thermally indirect motions in the convective atmospheric boundary layer, Journal of the Atmospheric Sciences, **40(2)**, 343-358, 1983.

https://doi.org/10.5194/angeo-2020-91
Preprint. Discussion started: 13 January 2021

Annales Geophysicae Discussions
Open Access
EGU

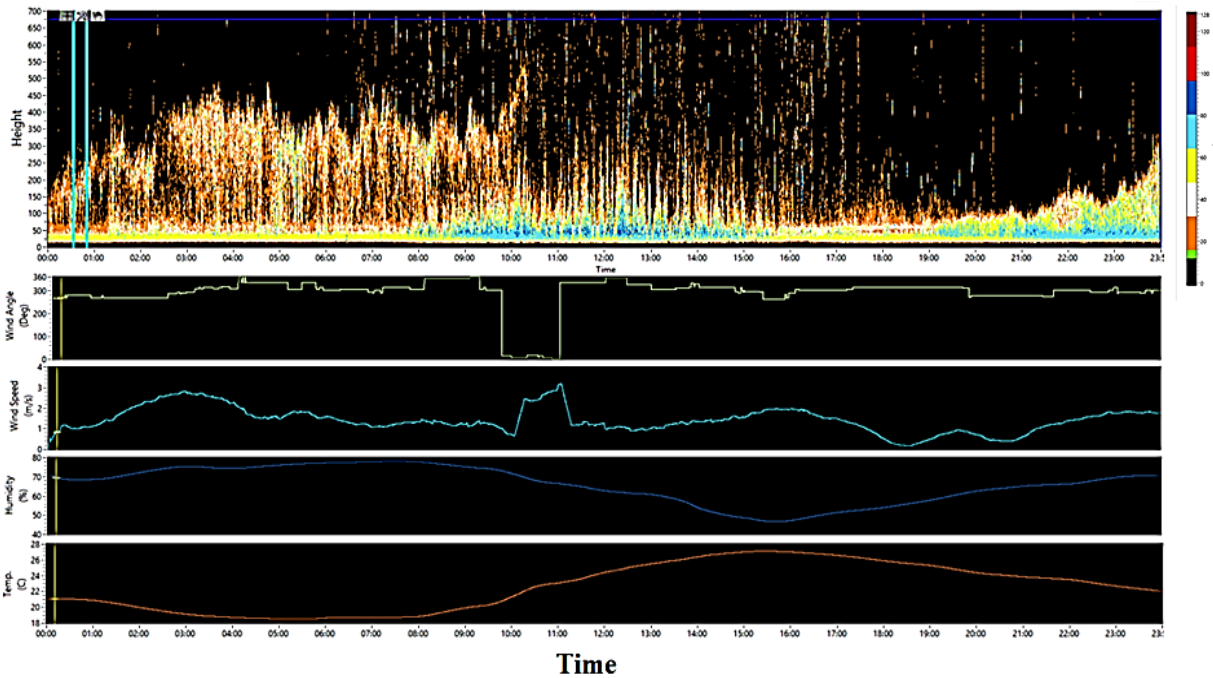

Figure 1 Temporal Variation of Atmospheric boundary layer

https://doi.org/10.5194/angeo-2020-91
Preprint. Discussion started: 13 January 2021

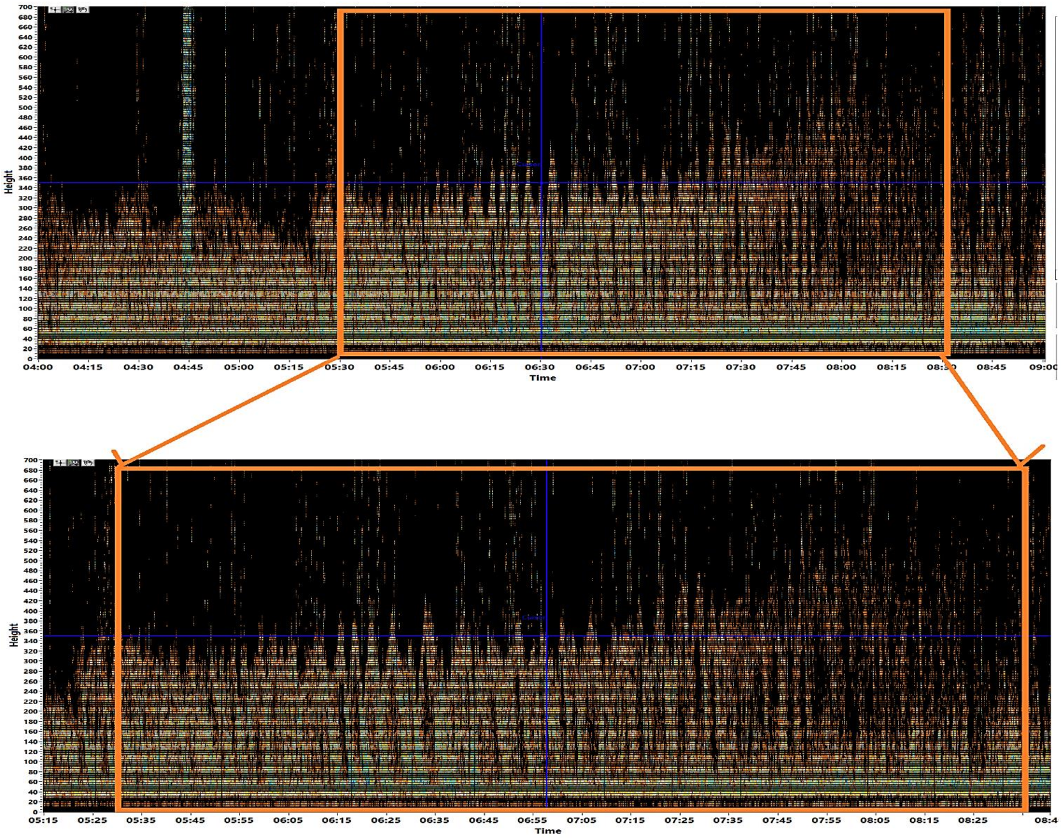

Figure 2. Features of the Parameters for KHBs Episode, ABL May 19, 2019 (for 3 hours)

https://doi.org/10.5194/angeo-2020-91
Preprint. Discussion started: 13 January 2021

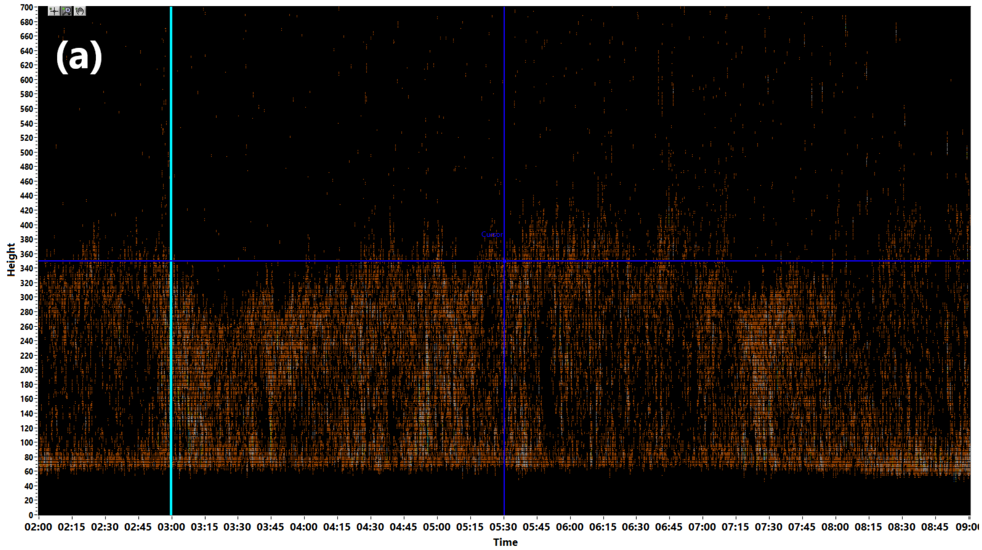

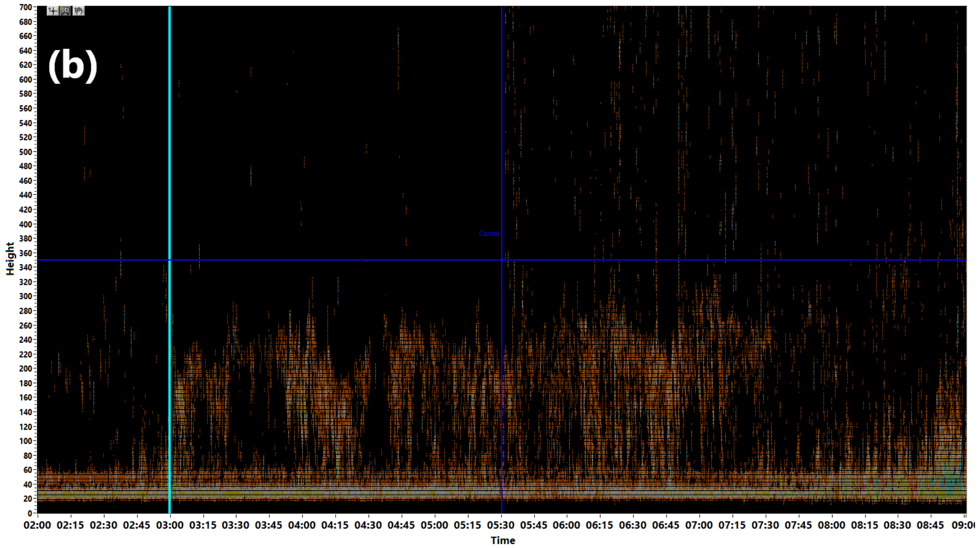

https://doi.org/10.5194/angeo-2020-91
Preprint. Discussion started: 13 January 2021

Annales Geophysicae Discussions
Open Access

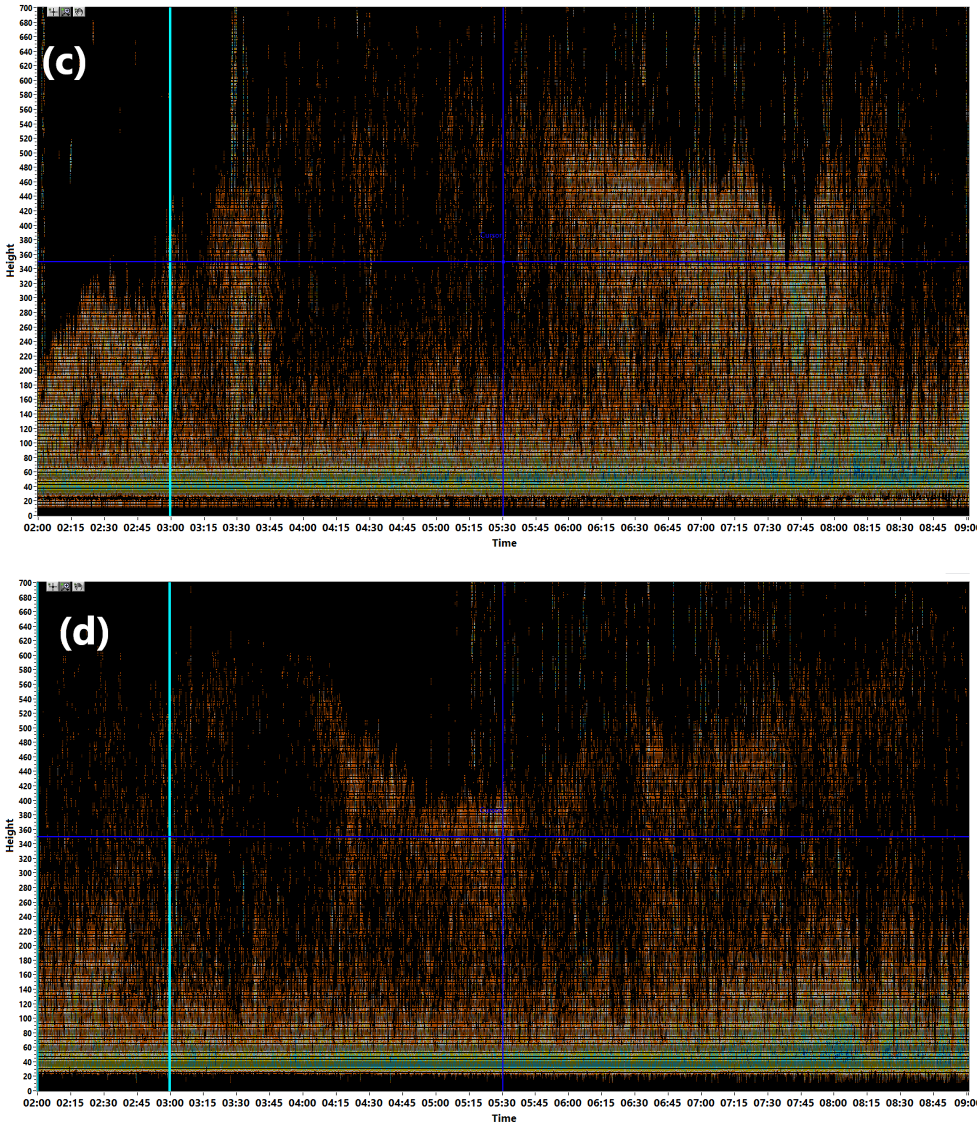

Figure 3. SODAR visualization of KHBs within Elevating Inversion Layers (for 7 hours) (a) 12th March 2019, (b) 26th April 2019, (c) 25th May 2019, (d) 14th June 2019

https://doi.org/10.5194/angeo-2020-91
Preprint. Discussion started: 13 January 2021

Annales Geophysicae Discussions

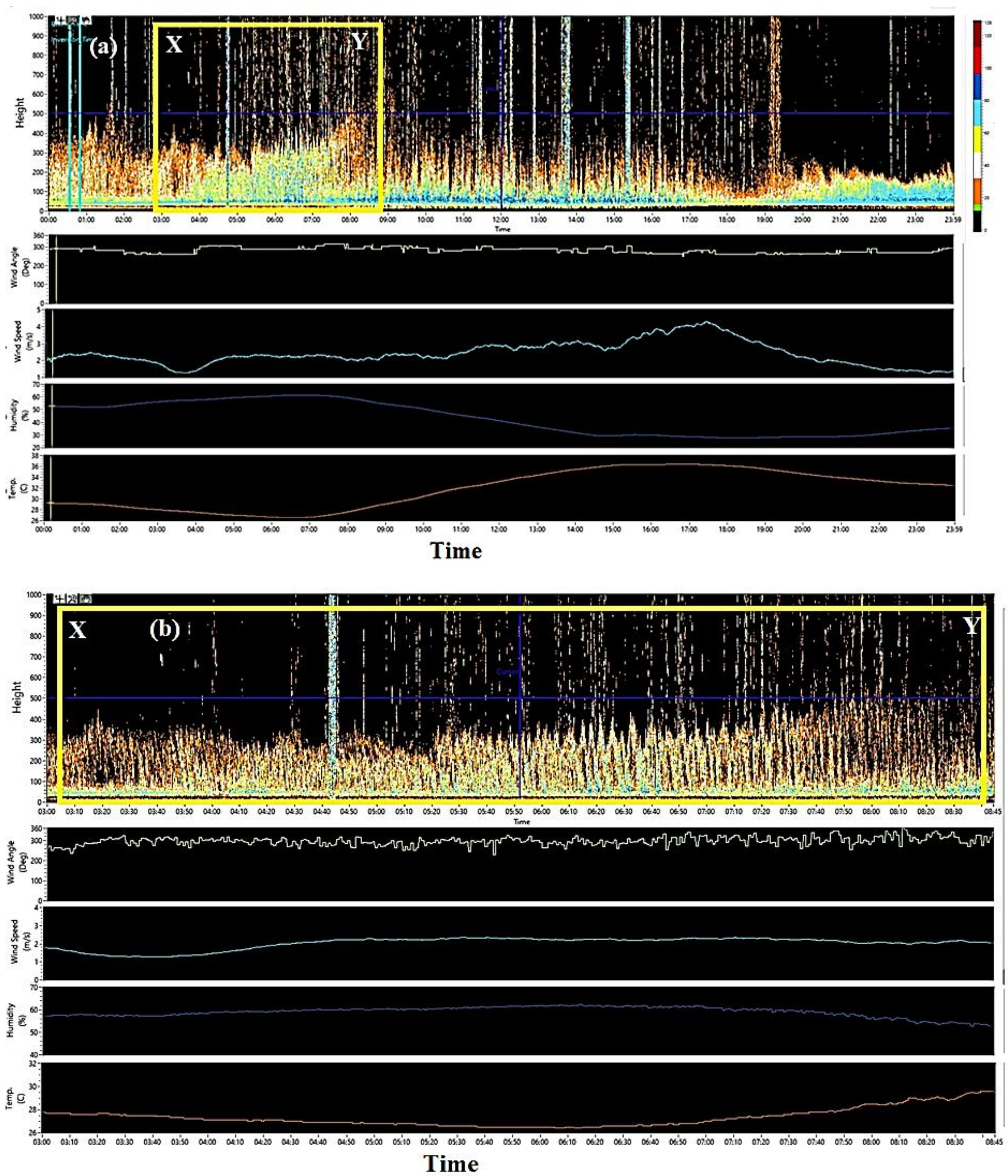

Figure: 4 Temporal variation of ABL height during KH billows with meteorological parameters (a) ABL for 24 hours, (b) ABL height during KH Billows (from 03:00 to 8:45)

https://doi.org/10.5194/angeo-2020-91
Preprint. Discussion started: 13 January 2021

Annales Geophysicae
Discussions

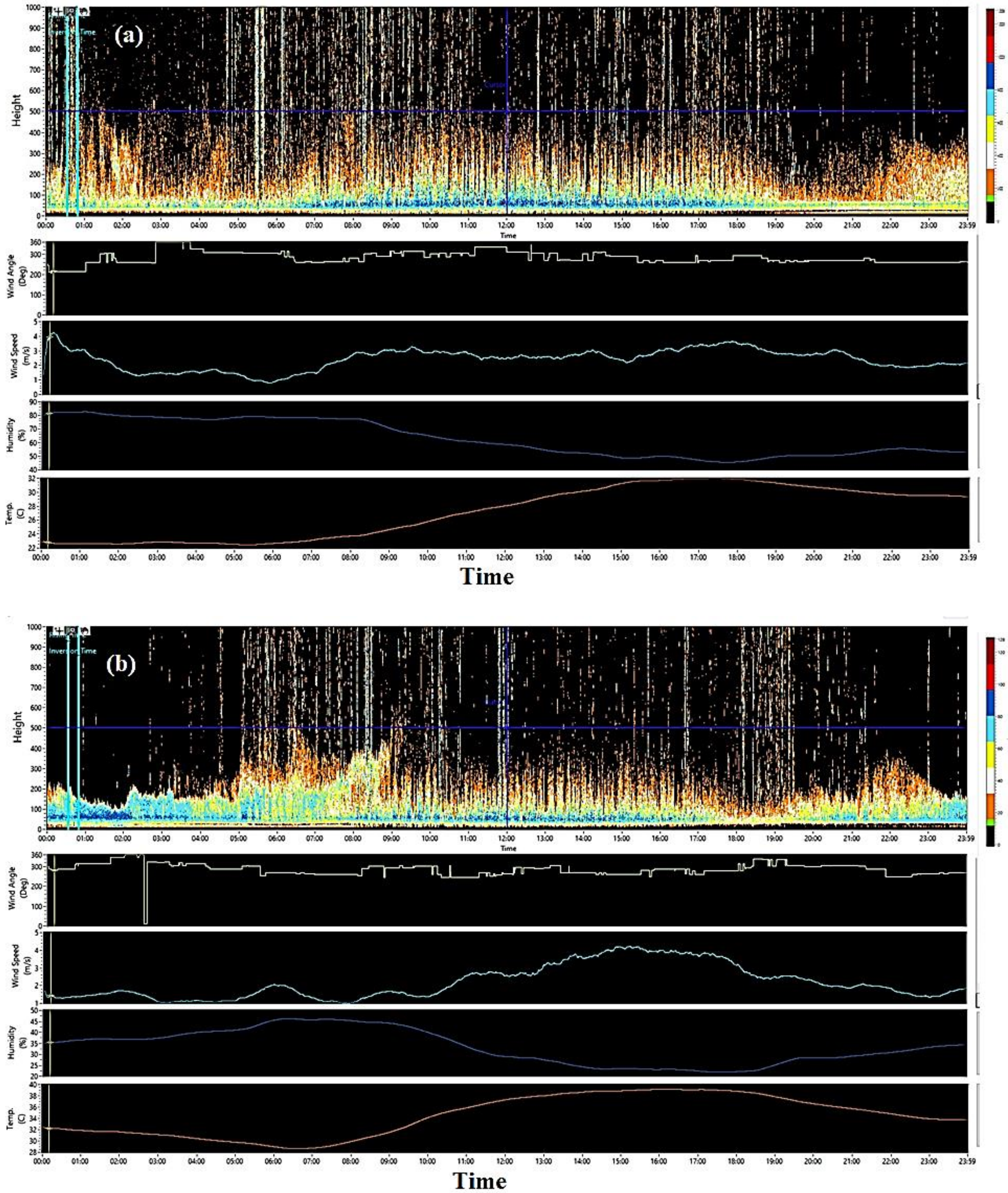

Figure: 5 Temporal variation of ABL height before KH billows with meteorological parameters (a) 18 May 2019 (Pre KH billows day), (b) 20 May 2019 (Post KH billows day)